Journal of Physics: Conference Series

PAPER • **OPEN ACCESS**

Interaction between Free-Stream Turbulence and Tip-Vortices of Wind Turbine Blades with and without Winglets

To cite this article: A. Al-Abadi *et al* 2018 *J. Phys.: Conf. Ser.* **1037** 072025

View the article online for updates and enhancements.

Related content

- Analysis of winglets and sweep on wind turbine blades using a lifting line vortex particle method in complex inflow conditions
  Matias Sessarego, Néstor Ramos-García and Wen Zhong Shen
- Fast trailed and bound vorticity modeling of swept wind turbine blades
  Ang Li, Georg Pirrung, Helge Aa. Madsen et al.
- Finite Element Analysis for the Web Offset of Wind Turbine Blade
  Bo Zhou, Xin Wang, Changwei Zheng et al.



IOP ebooks™

Bringing you innovative digital publishing with leading voices to create your essential collection of books in STEM research.

Start exploring the collection - download the first chapter of every title for free.

This content was downloaded from IP address 178.237.49.162 on 27/03/2019 at 11:03

Interaction between Free-Stream Turbulence and Tip-Vortices of Wind Turbine Blades with and without Winglets

A. Al-Abadi[1], Y. Kim[2], Ö. Ertunc[3], P. Epple[4], and A. Delgado[2]

[1]SGB Power Transformers (SGB-SMIT Group), R&D, Regensburg, Germany
[2]Institute of Fluid Mechanics, Friedrich-Alexander-University, Erlangen, Germany
[3]Ozyegin University, Mechanical Engineering, Istanbul, Turkey
[4]Coburg University of Applied Sciences, Mechanical Engineering, Coburg, Germany

ali.al-abadi@sgb-smit.group

Abstract. Experimental investigations of the free-stream turbulence impact on the tip-vortices generated in wind turbine blades have been performed. The investigation is done by exposing an efficient laboratory scale wind turbine to different turbulence levels generated by two static grids installed in the cross section of a wind tunnel. Different winglet configurations to figure out the optimum design that can prevent the tip induced flow are studied. The power gained when adding different winglets is measured when exposing the turbine to turbulence. It is found that the strength of the vortices is reduced depending on the turbulence levels. Furthermore, higher power extraction associated with more expansion of wake and wake-border is shown. This is an indication for increasing of the mixing between the free-stream and the wake. Tip-vortex analysis of high turbulence levels has shown additional interaction of large-eddy scales contained in the free-stream turbulence. The turbulence helps to suppress the tip vortices, and thus, reduces the tip losses. Further investigations of the near and far wake-surrounding intersection are performed to understand the energy exchange and the free stream entrainment that help in wake recovery.

1. Introduction

Wind turbines normally operate under stochastic environments. Nevertheless, they are designed using the aerodynamic theory for a uniform ideal flow without turbulence. Hansen and Madsen [1] described the development of the aerodynamic tools that estimate the loads on wind turbines. As a result, the operating performance predicted will in general not correspond to the real performance. Wake characteristics and tip-vortices are two important parameters affected the performance of the wind turbines. Understanding the impact of the different levels of turbulence on the tip-vortices can deliver useful information for the design and performance prediction of efficient predicting of the Horizontal Axis Wind Turbines (HAWTs). Several researchers have studied the impact of the atmospheric turbulence on the performance of wind turbines. It has been shown that both power output and loads on turbine blades increase with increasing turbulence intensity levels, [2–3]. For a better prediction of the total power output of a HAWT, the evolution and the stability of the tip-vortex were investigated

Content from this work may be used under the terms of the Creative Commons Attribution 3.0 licence. Any further distribution of this work must maintain attribution to the author(s) and the title of the work, journal citation and DOI.
Published under licence by IOP Publishing Ltd

experimentally [4]. The tip-vortex behavior at a high tip speed ratio was investigated, Whale and Anderson [5], whereas Wood [6] was showed that the fundamental behavior of the helical vortex wake is insensitive to blade chord Reynolds number, when the tip speed ratio is in dynamical similarity. Tip-vortices have a major importance in wake investigations since they behave as a shield preventing the wake from mixing with the free stream flow. Thus, changing their structures has a strong influence on the wake, and hence on the power output of a HAWT. The effects of winglets in wind turbines have been investigated with CFD-RANS simulations in order to enhance the aerodynamic performance of the wind turbine [7, 8].

In the present study the impact of turbulence on the tip-vortices as well as the interaction of different turbulence scales with the tip-vortices were investigated. The influence of turbulence on the breaking down and hence mitigation of the wake border was studied in order to understand the effect of the mixing between the free-stream and the wake on the performance of a HAWT. The investigation was done by exposing an efficient wind turbine model to different turbulence levels generated by two static grids installed in the cross section of a wind tunnel.

2. Experimental Investigations

For the experimental investigation of the impact of the free-stream turbulence on the tip-vortices of the HAWT blades, an optimized laboratory scale wind turbine was developed by using the TMASO method. TMASO is an optimization method that changes the blade shape in order to capture the maximum power from the wind under the torque-rotational speed constraint of the drive unit. The method is called as Torque Matched Aerodynamic Shape Optimization (TMASO) [9]. The TMASO method delivers feasible results for an efficient turbine that can also be up-scaled to the size of a large scale HAWT. The measurements were conducted in the closed loop wind tunnel of the Institute of Fluid Mechanics of the University of Erlangen-Nuernberg (LSTM) by exposing the wind turbine to turbulence of various levels and length scales. Details of the wind turbine setup that consists of rotor, generator, mechanical tower, nacelle and electrical circuitry are explained in [10, 11].

The turbulence is generated by using two static grids with a fine (8mm) and coarse (40mm) spacing, Figure 1. Hence, two completely different turbulence scales are obtained at the inlet of the wind tunnel. The turbulence is nearly isotropic and decays in the flow direction, Figure 2. The turbulence isotropy was measured in prior investigations for the same wind tunnel and the same grids [12].

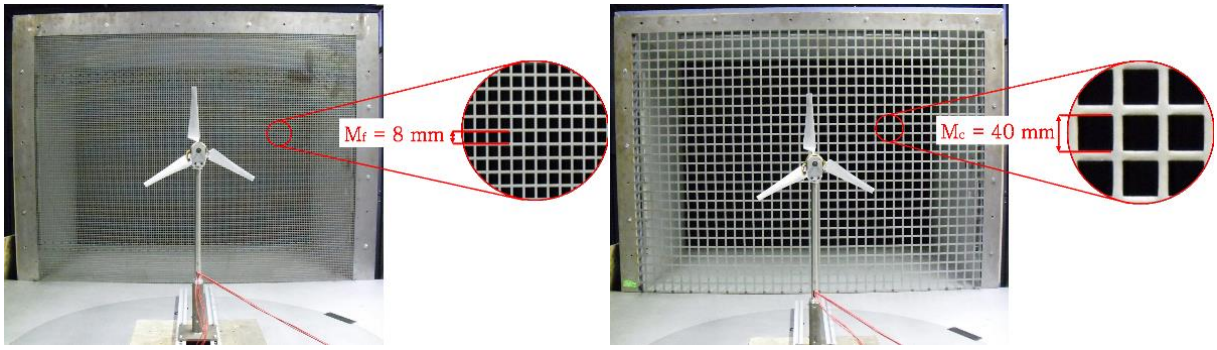


Figure 1: Optimized wind-turbine exposed to two grids (fine and coarse grids) in the wind tunnel.

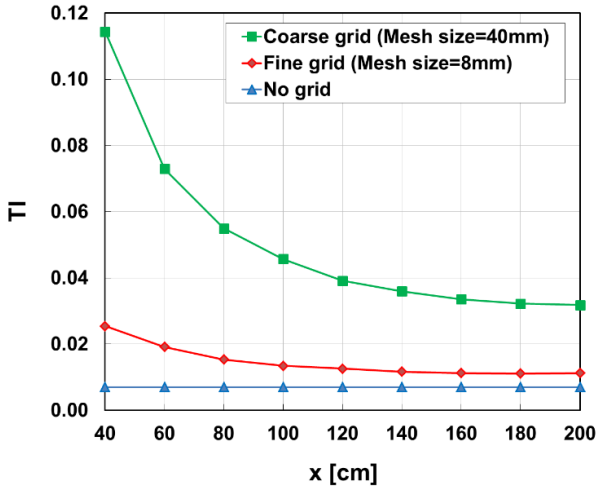


Figure 2: Intensity of grid-generated turbulence along the test section for the three cases (no grid, fine and coarse grids).

A Pitot-static tube was fixed on a 3-D traversing system alone for the velocity measurements, and beside a hotwire probe for calibration. The velocity measurements were performed by measuring the difference in static and total pressure with a SETRA differential-pressure transducer connected to the Pitot-static tube and by applying the Bernoulli equation.

To measure the velocity fluctuations and hence the turbulence level, a single normal hot-wire connected to an anemometer unit with a constant-temperature bridge CTA was employed. The wire has a length of 1mm and a diameter of 5µm. A velocity calibration of the employed hot-wire probe was performed at the test section near the inlet of the wind tunnel test section. During the calibration and the measurements, the temperature of the flow was measured with a PT100 temperature sensor to correct the measured data for temperature drifts. The hot-wire signals, the pressure transducer signal and the temperature signal were acquired by a 16-bit A/D converter (NI 6059E DAQ card) installed in a personal computer. The data were recorded for further analyses of spectra and autocorrelation. The sampling rate (SR) for the measurements was chosen in such a way that wide scales of fluctuations can be acquired. The sampling rate SR was set to 20 kHz, with an overall measuring time period of t=120s. Thus, the acquired 2.4 million data can provide a wide range of turbulence scales and a certainty of the turbulence intensity (TI) measurement, which is determined experimentally in the present study by increasing the SR until convergence of the TI. Those measurements were conducted with hot-wire anemometry in the absence of the wind-turbine. The facility allows exposing the wind turbine to turbulence with various energy and length scale levels.

The reference wind speed was set to the free-stream velocity of v1=12m/s, which is the design speed for the turbine model. Measurements of velocity were taken in an area around the tips at the normalized axial distances of x/D=0.2, 0.4 and 0.6. For each x/D, the radial direction with the highest fluctuation in velocity was chosen and directly compared to the corresponding y/D for different turbulence levels. Figure 3 shows the non-dimensionalised upwind velocities. It is clear from the figure 3 that the required distance to measure the reference upwind velocity is function of turbulence level (since the rotational speed and hence the blockage effect of the wind turbine is different for the three investigated cases). The distance lies in the range of -1.3, -1.1 and -0.9 (x/D: upwind distance to diameter ratio), for the three cases without grid, with fine grid and with coarse grid, respictively. The measurement for the power coefficient will be taken when the wind turbine model is mounted at 120 cm distance from the wind-tunnel test-section entrance (For the worst case: 1,3*50 cm (diameter)=65 cm). Figure 4 shows the measurement positions within the total experimental setup.

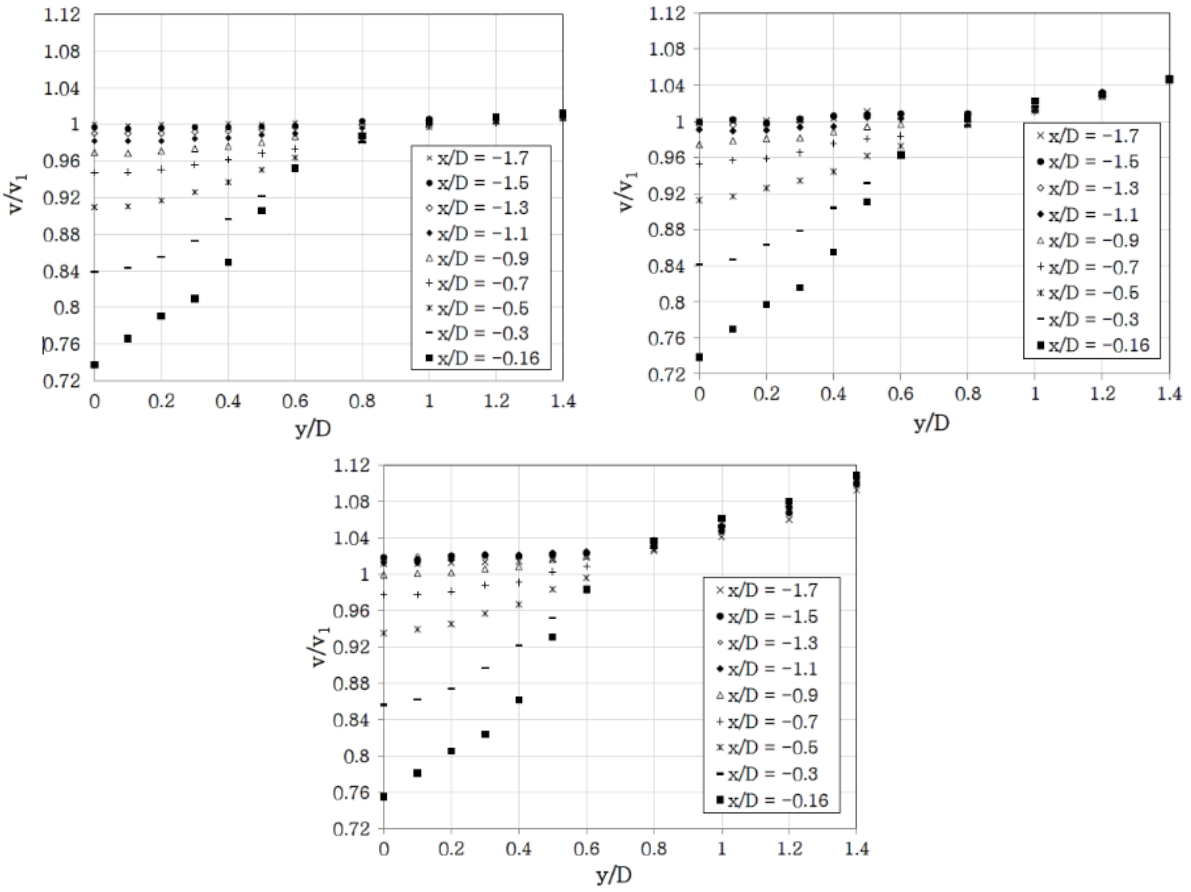


Figure 3: Upwind velocity distribution (non dimensionalized to v1=12 m/s) (a) without grid, (b) with fine grid, (c) with coarse grid

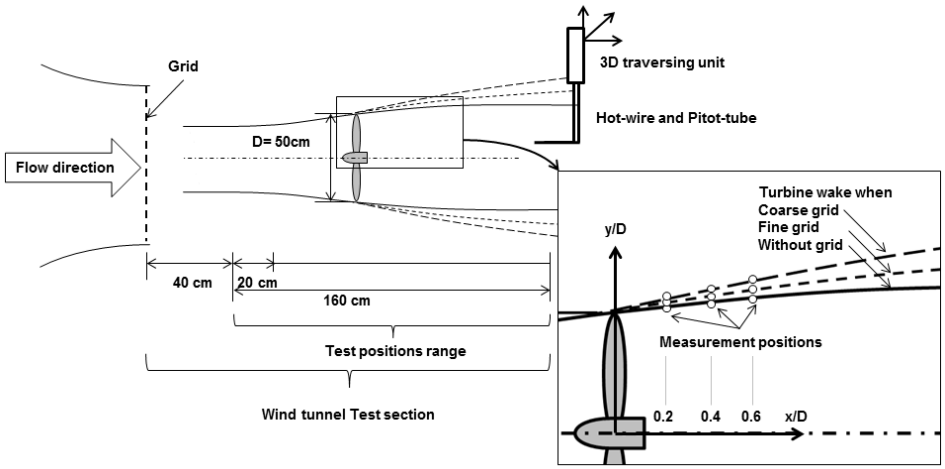


Figure 4: Experimental set-up and the measurement positions.

The energy spectrum at a hot-wire probe distance from the grid of x=120cm at the design free-stream wind velocity is depicted in Figure 5. The position of x=120cm was selected since it satisfies both the isotropy of the free-stream turbulence and a sufficient down-stream distance for wake and

hence tip-vortices development. Furthermore, the turbulence length scale of the freestream turbulence is shown in Figure 6 for both cases, for the fine and for the coarse grid.

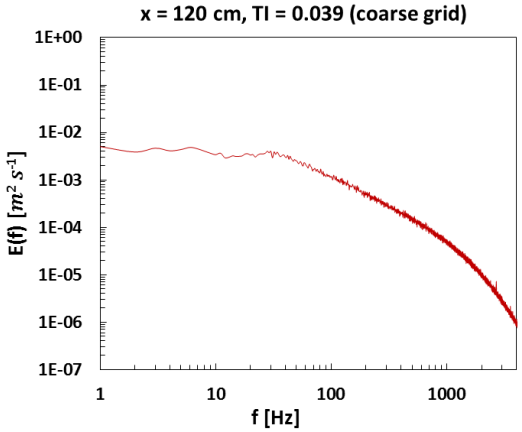


Figure 5: Distribution of Spectra E(f) with eddies frequencies f when using the coarse-grid at the design free-stream wind velocity of v1=12 m/s, turbulence intensity of TI=0.039 and hot-wire position of x=120 cm with the absence of wind turbine.

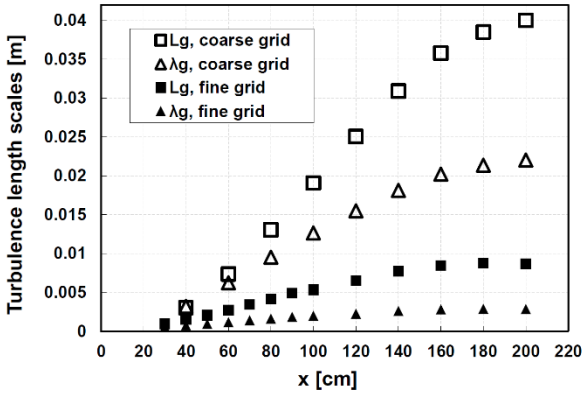


Figure 6: Turbulence length scales distribution along the test section when using fine grid and coarse grid (Lg: Integral scale, λg: Taylor scale).

3. Tip Vortex Analysis

As shown in Figure 7(a), the maximum fluctuation for the free-stream low turbulence (without grid) happens at an axial distance of x/D=0.2 and a radial distance of y/D=0.52. Here, the influence at medium (with fine grid) and high turbulence (with coarse grid) levels are not at their maximum yet. With increasing turbulence intensity, the downstream velocity decreases. Thus, the wake becomes wider, which indicates a higher power extraction. Measured velocities are less than the reference velocity v1=12 m/s for all cases, because the measurements were taken inside the wake of the turbine. There is a second kind of fluctuation recognizable; it can be clearly seen for the coarse grid case, which is due to the high turbulent scale eddies.

As can be seen in Figure 7(b), when moving in the radial direction of $\Delta y/D = 0.01$ to reach y/D=0.53, there is an enormous jump in velocity. This position is outside the wake for the low turbulence case, but still inside for medium and high turbulence levels. This means, the medium and high turbulent wakes are wider than the low turbulent one. Counting 32 maximums peaks within a period of t=1s leads to an angular speed of w=200rad/s, which indicates that these fluctuations is directly related to the rotor tips. At this position, the fluctuation is at maximum for the fine grid case. At a radial distance of y/D=0.54, there is maximum fluctuation for the high turbulence case with the coarse grid. The result is shown in Figure 7(c). Here, it is not exactly clear, if the high turbulence measurement was taken inside or outside of the wake since the accuracy of the traversing system is limited to 5mm. It is possible that it was somewhere in between, but for low and medium turbulence cases it is very clear. Again, here the influence of the tips is still. While with the use of the fine grid, there is an explicit influence of the mixing of the turbulence eddies and there is no influence at all for the low turbulence case.

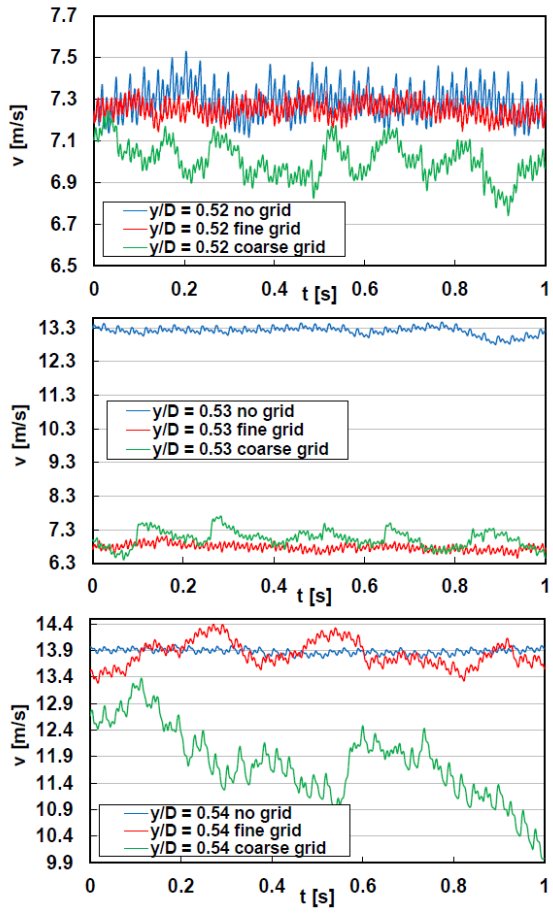


Figure 7: Tip vortices at x/D=0.2 for different turbulence levels (a) y/D=0.52, maximum fluctuation without grid, (b) y/D=0.53, maximum fluctuation with fine grid, (c) y/D=0.54, maximum fluctuation with coarse grid.

At the axial position of x/D=0.4, the radial position with maximum fluctuation for the low turbulence case is at y/D=0.56, as shown in Figure 8(a). In comparison to the x/D=0.2, the steam tube is wider. This is true since we have moved in the downstream direction. The absolute fluctuation decreases a bit and there is more mixing inside the wake, since there are different eddy scales mixing themselves with the tip vortices. The same situation happens in a more pronounced way as shown for the fine and the coarse grid. Here, the Pitot-tube was again placed inside the wake. In contrast, for the distance of y/D = 0.57, the low turbulence vortices are outside the wake, as shown in Figure 8(b). The number of maximum peaks counted hare about 33. This means, the angular velocity w=206rad/s, which is higher than in the case without grid. For the high turbulent case, the number is even higher. This indicates an increase of the angular speed with the increment of turbulent levels.

It can be seen in Figure 9(a) that the mixing area is wider. The velocity in the low turbulent case drops to an average of approximately 11m/s. For the fine and the coarse grid, a substantial influence of the mixing with the surrounding wind is shown. The gap between the expansions of the stream tube becomes wider with higher x/D distances from the rotor plane. Moving with Δy/D=0.02 outside, Figure 9(b), the maximum fluctuation of the fine grid is the same as the coarse grid. The difference between both in mixing and velocity is more pronounced.

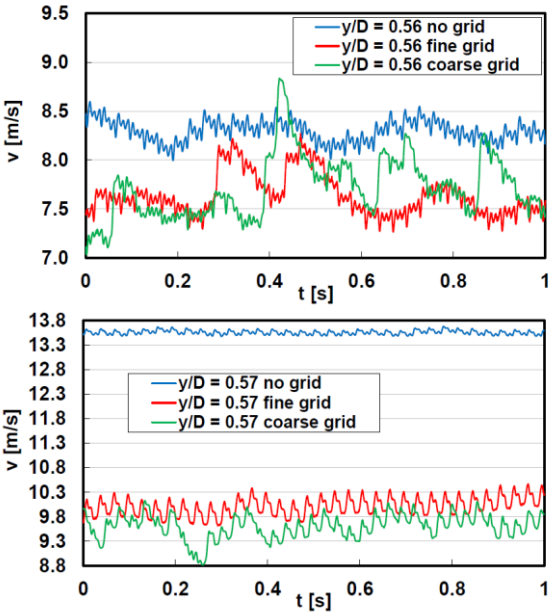


Figure 8: Tip vortices at x/D=0.4 for different turbulence levels (a) y/D=0.56, maximum fluctuation without grid, (b) y/D=0.57, maximum fluctuation with fine and coarse grids.

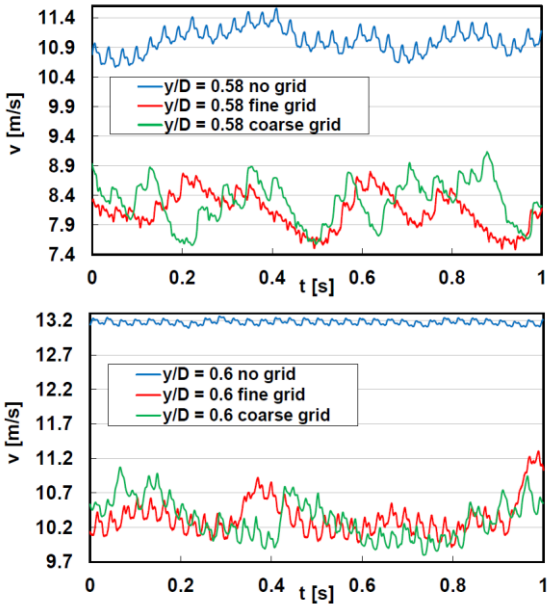


Figure 9: Tip vortices at x/D=0.6 for different turbulence levels (a) y/D=0.58, maximum fluctuation without grid, (b) y/D=0.6, maximum fluctuation with fine and coarse grids.

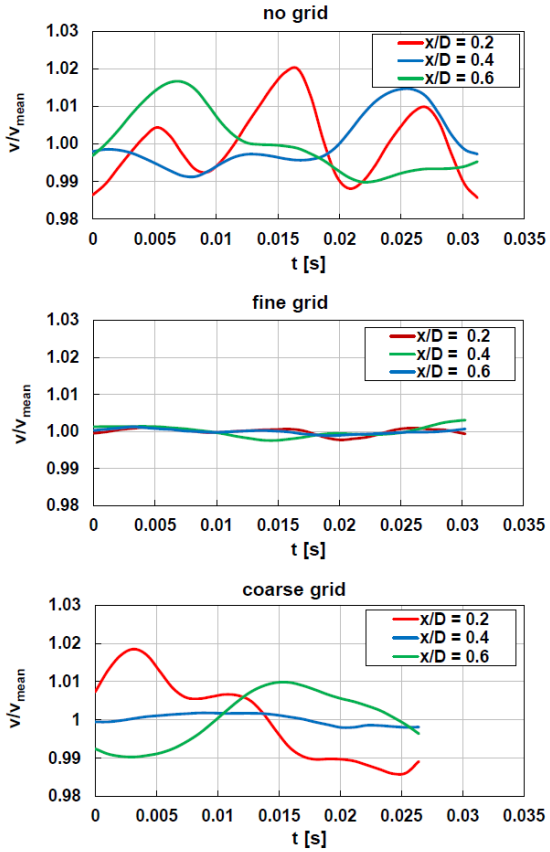


Figure 10: Comparison of the tip vortex for a single revolution of the rotor at varying x/D and turbulence level

The one revolution maximum tip vortex is obtained by splitting the tip-vortices into the corresponding frequency values which is known from the angular speed ω of the three cases (where, f=ω/2π). Then, the set of data were averaged to obtain only one rotational averaged vortex. The velocity is normalized by its mean value to simplify the comparison. For a full revolution, three tips are expected to be seen. Each minimum appears when a rotor blade is passing in front of the Pitot-tube, Figure 10. It can be clearly seen that not only the tip vortices are damped in amplitude with increasing turbulence, but also the revolution speed increases (less time). At the same time the mixing with the surrounding increases. Figure 10(b) shows that vortices are suppressed for the case of the fine grid, despite that, the peaks of the vortex are still appearing. In contrast, the coarse grid case Figure 10(c), the additional damping delays until the distance of 0.4, where there are no clear vortex peaks. There is only a higher mixing with the large eddy scales containing in the incoming turbulence.

4. Winglet Effect

To isolate the major influence of the tip-vortex from other factors that possibly contribute to the performance increment, winglets were mounted at the tip of the rotor blades. Winglets are supposed to reduce the tip losses by preventing the flow across the tip and result in higher power extraction. Thus, different designs were tested until reaching a noticeable power increment Figure 11.

Figure 12 shows the increment of the power coefficient ($C_P = P_{shaft}/P_{wind} = 0.5\ \rho v^3 A$, [13]) when using winglet compared to the measurement without winglets at different turbulence levels. The gain when adding winglets can be seen very clearly. This difference, however, is still smaller than when exposing the turbine to turbulence generated by grids, the fine and the coarse grids. Hence, preventing tip-vortices is not the sole reason for the increment of C_P with the increase of turbulence levels. There might be additional possibilities for that increment. Turbulence not only helps in suppressing the tip vortex, but there are additional possible effects.

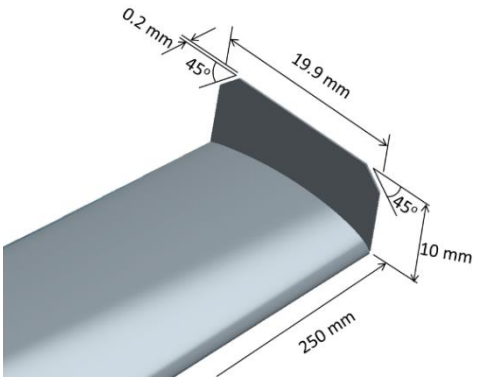


Figure 11: Optimum winglet design.

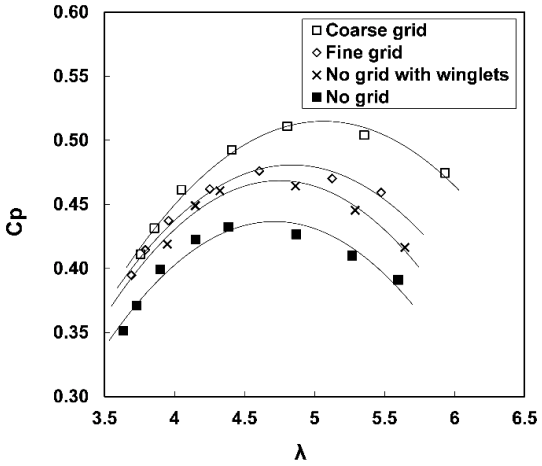


Figure 12: The effect of winglet on the C_P at free flow turbulence in comparison with the turbulence.

5. Spectrum Analysis

The spectrum analysis is used to highlight more details of the impact of turbulence on the tip-vortices structures, and hence, the free-stream wake interaction at different turbulence levels. Starting with the near wake distance at x/D=0.3, Figure 13 shows the case when the turbine is mounted at a test section position of x=100cm from the inlet of the test section, where the incoming turbulence intensities (TI) are 0.007, 0.013 and 0.046 for the no grid, fine grid and coarse grid cases, respectively. It is possible to distinguish between energy developments as a function of eddy frequencies f at a different incoming TI.

In general, the energy of the most energy containing frequencies (f<100Hz) increases. This increment is associated with the penetration of the incoming turbulence through the rotor plane (between the blades). Figure 13 also shows three distinguished jumps of the energy at defined frequencies (f=34, 66 and 100Hz). These peaks are more apparent at a measurement position of y/D=0.4, and they correspond to the three rotor blades and represent the additional increment of TI (and thereby turbulent energy) of the rotation of the turbine. As expected, the amplitude decays with increasing distance from the tip at y/D in both directions. Here, the mixing is most distinctive. With additional incoming grid-generated turbulence, the turbine rotates faster. This fact becomes clear in the Figure 13 by the shift of the peaks to higher frequencies. Especially at the maximum fluctuation position for the low turbulent case, there is a high intensive mixing over a wide interval of frequencies. The effect fades with higher incoming turbulence, for the high turbulent case it disappears nearly completely. The fading is also noticeable for increasing measuring distance from the turbine Figure 14. Here, the three typical peaks still exist, but tip vortices vanish due to dissipation.

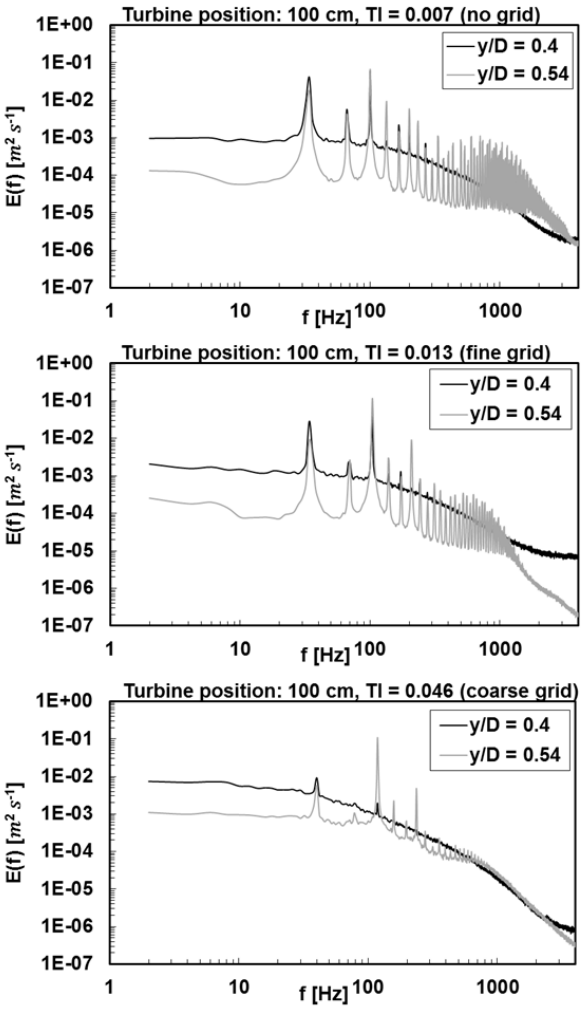


Figure 13: Distribution of Spectra E(f) with eddies frequencies f at different radial distance y/D in the turbine wake for different free-stream turbulence levels at hot-wire in downwind position of x/D=0.3.

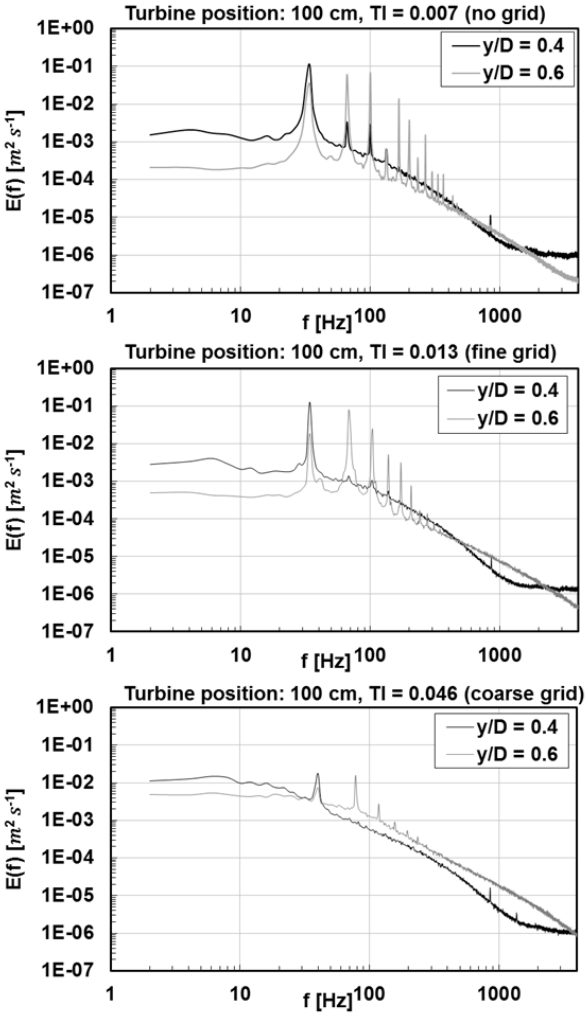


Figure 14: Distribution of Spectra E(f) with eddies frequencies f at different radial distance y/D in the turbine wake for different free-stream turbulence levels at hot-wire in downwind position of x/D=1.1.

6. Conclusions

The present study presents the impact of wind turbulence on the performance of the HAWT via investigating the interaction of the free-stream turbulence with the tip-vortices. Result shows that with optimization of the rotor blades and additional tip-winglets there is a high potential of extracting more power by the turbine when exposed to higher level of turbulence for the same reference upwind velocity. Explanation is that the turbulence helps in suppressing the tip-vortices and therefore, reduces the tip losses. Tip-vortices forming barrier cone behind the wind turbine that preventing the mixing between the free-stream and the wake. Therefore, suppressing it enhances of the mixing, and hence, faster wake recovery is achieved. Furthermore, the study shows a penetration of the free-stream turbulence through the rotor plane (between the blades), which helps in energizing the wake with large eddies of the upwind flow and hence reduces its adverse pressure effect. Adding winglets to the blade tip reduces the tip-vortices and hence isolates a major part of it. The power gain when adding winglets is less than when exposing the turbine to turbulence. Hence, preventing tip-vortices is not the sole reason for the increment of power.

References

[1] Hansen, M. O. L., and Madsen, H. A., 2011, "Review Paper on Wind Turbine Aerodynamics," ASME J. Fluids Eng. 133(11), 114001. doi:10.1115/1.4005031

[2] Hansen, K. S., Barthelmie, R. J., Jensen, L. E., and Sommer, A., 2012, "The impact of turbulence intensity and atmospheric stability on power deficits due to wind turbine wakes at horns rev wind farm" Wind Energy, 15(1), pp. 183–196. DOI: 10.1002/we.512

[3] Türk, M., and Emeis, S., 2010, "The dependence of offshore turbulence intensity on wind speed," Journal of Wind Engineering and Industrial Aerodynamics, 98(8-9), pp 466-471.

[4] Odemark, Y., 2012, "Wakes behind wind turbines studies on tip vortex evolution and stability," Internal report, Royal Institute of Technology KTH Mechanics. ISSN 0348-467X. ISRN KTH/MEK/TR--12/06--SE

[5] Whale, J., Anderson, C., Bareiss, R., and Wagner, S., 2000, "An experimental and numerical study of the vortex structure in the wake of a wind turbine," Journal of Wind Engineering and Industrial Aerodynamics, 84(1), pp 1-21.

[6] Wood, D. H., 1998, "The velocity of the tip vortex of a horizontal-axis wind turbine at high tip speed ratio," Renewable Energy, 13(1), pp. 51-54.

[7] Johansen, J., and Soerensen, N., 2006, "Aerodynamic investigation of winglets on wind turbine blades using cfd," Risoe-R Report.

[8] Gaunaa, M., and Johansen, J., 2007, "Determination of the maximum aerodynamic efficiency of wind turbine rotors with winglets," J. Phys.: Conf. Ser. 75 012006. doi:10.1088/1742-6596/75/1/012006

[9] Al-Abadi, A., Ertunc, Ö., Beyer, F., and Delgado, A., 2014, "Torque-matched aerodynamic shape optimization of HAWT rotor," J. Phys.: Conf. Ser. 555 012003. doi:10.1088/1742-6596/555/1/012003

[10] Al-Abadi, A., Ertunc¸, Ö., Epple, P., Koerbel, W., and Delgado, A., 2012, "Development of an experimental setup for double rotor HAWT investigation, " ASME Turbo Expo 2012: Turbine Technical Conference and Exposition, 6, pp. 1007-1016. ISBN: 978-0-7918-4472-4. doi:10.1115/GT2012-70032

[11] Al-Abadi, A., Ertunc¸, Ö., Weber, H., and Delgado, 2014, "A torque matched aerodynamic performance analysis method for the horizontal axis wind turbines," Wind Energy, 17(11), pp.1727-1736. DOI: 10.1002/we.1664

[12] Ertunc, Ö., 2006, "Experimental and numerical investigations of axisymmetric turbulence," PhD thesis, https://opus4.kobv.de/opus4-fau/frontdoor/index/index/docId/398

[13] Manwell, J. F., McGowan, J. G., and Rogers, A., 2002, "Wind Energy Explained: Theory, Design and Application," John Wiley and Sons, Ltd.